

Multi-sensor blue LED and touch probe inspection system

Kai Xue , Venu Kurella  and Allan Spence 

McMaster University, Canada

ABSTRACT

In coordinate metrology, features of sheet metal parts in early production may be significantly out of nominal, so the inspection path created from its CAD nominal has to be adjusted to avoid cosine error or probe collisions. To solve this problem and seize the advantages of contact and non-contact measurement methods, a multi-sensor blue LED scanner and touch-trigger inspection system was constructed, in which the tactile inspection path was tuned by scanner data. Extrinsic calibration of the scanner was investigated using an angled slot target. Additionally, a lightweight 2-axis rotary table was designed for use with surfaces with non-vertical normal directions. The calibration, qualification, registration, and path correction methods are presented. A stamped sheet metal automobile part was experimentally measured.

KEYWORDS

Multi-sensor inspection;
structured light;
touch-trigger probe

1. Introduction

Coordinate metrology plays an important role in quality management and process control [20]. With new developments in production, the requirements for innovative metrology methods and techniques become increasingly diverse. Contact and non-contact measurement methods each have their own respective strengths and weaknesses [2],[19]. Touch-trigger probes can achieve low uncertainty [7], and perform well inside deep holes, but have limited data acquisition speed. Moreover, soft material surfaces may deform when touched. In contrast, non-contact digitizers collect high density surface point clouds in seconds, and are much less likely to suffer from sensor collisions with the part, but have higher uncertainty, and are constrained by visibility and specular reflection difficulties. Therefore, researchers have investigated all inclusive part surface measurement using multi-sensor metrology. Multi-sensor metrology combines non-contact digitizers and touch probes, usually on a Coordinate Measuring Machine (CMM). This sensor integration has made it possible to measure almost all kinds of features that may not be obtained by one sensor or the other alone. The high measuring speed of multi-sensor CMMs enables economical on-line inspection [6].

Two kinds of information interaction between the outputs from multiple sensors can be observed in related research, i.e., complementary interaction and synergistic interaction [12]. Complementary information interaction means two or more sensors digitize different features

of the same object that are independent of each other. Synergistic information interaction occurs when the data obtained by one sensor (optical scanner) can guide the inspection path of another sensor (touch probe). Different multi-sensor measurement systems have been implemented by researchers, but their research has a different focus and methods. Zhao et al. [23] and Mohib et al. [11] focused on computer-aided inspection planning. They used their systems in a complementary way. Sladek et al. [18] and Xie et al. [22] combined a structured light vision system and a touch probe by complementary interaction as well. The vision system was composed of a digital projector and a Charge-Coupled Device (CCD) camera. A one-axis rotary table was used in Xie's research. In Nashman et al.'s research [12], synergistic interaction was implemented using a video camera and an analog touch probe. The camera captured both the feature of the object and the touch probe stylus. Distance between the point to be measured and the touch probe was calculated by image processing. Although there were both complementary and synergistic interactions in Shen et al.'s research [16], the projector and the camera of the vision system required time consuming separate calibration.

A long standing problem in tactile measurement is the situation when features of sheet metal parts produced at early production stage significantly deviate from nominal. Consequently, Dimensional Measuring Interface Standard (DMIS) inspection paths created using the CAD nominal geometry can no longer be used without

introducing significant part surface cosine error. In more extreme cases, missed touches or probe collisions can occur. Existing methods for solving this problem have included taking preliminary sample points around the (hole or other) feature, and then iterating to obtain more accurate results.

To solve this more efficiently, a multi-sensor blue Light Emitting Diode (LED) structured light scanner and touch-trigger inspection system was developed and is reported in this paper. Both complementary and synergistic interactions were implemented in this system. Extrinsic calibration of the scanner was investigated using a designed angled slot target. The touch probe measurement path created from the CAD nominal was fine tuned after using the scanner data to estimate (hole) feature sizes and positions. A lightweight 2-axis rotary table was designed for use with surfaces with non-vertical normal directions. Three tooling spheres were fixed on the rotary table for coordinate system registration. The workpiece was scanned at different orientations, and the data patches were merged together.

The scanner integrates a Structured Light Modulator (SLM), a blue LED, and two cameras into one single device. When mounted on a CMM, the structured light

scanner is more convenient to use in terms of recording coordinates, as it can capture an entire 3D surface in view when standing still. Built-in measurement tools for 3D feature recognition are offered inside the sensor.

Section 2 describes the configuration of the multi-sensor system. In Section 3, the working principle of the system is introduced, including extrinsic calibration of the scanner, synergistic inspection, and oriented part inspection. Section 4 reports automotive sheet metal part measurement results. Section 5 concludes the paper.

2. Multi-sensor inspection system configuration

The components of this multi-sensor system (Fig. 1) are listed as follows:

- CMM: DEA IOTA-P with retrofitted motors and motion control computer.
- Head and touch-trigger probe: Renishaw® PH6/TP6 [13].
- Blue LED structured light scanner: Gocator 3110 [8].
- Counter card: PCI-QUAD04 four-channel quadrature encoder input board [9].
- Renishaw® AM1 adjustment module [13].

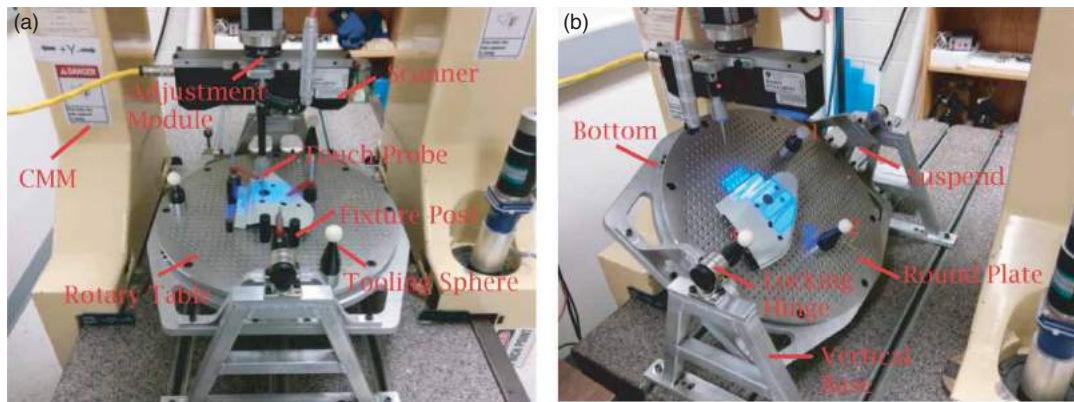


Figure 1. Multi-sensor system configurations: (a) Horizontal, (b) Oriented.

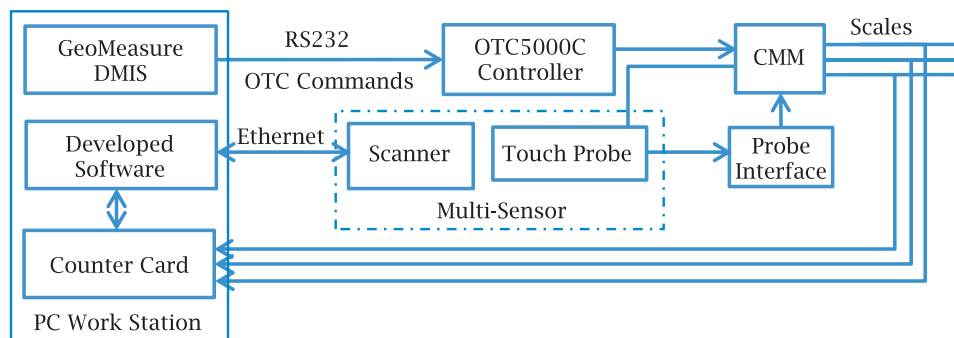


Figure 2. Connection between components of the system.

- Siemens NX 9.0 [17].
- Mitutoyo GeoMeasure 3000 DMIS interpreter software [10].
- Geomagic Qualify 12 3D reverse engineering software [5].

The connection between them is illustrated in Fig. 2.

For the CMM, the volumetric roll/pitch/yaw errors as a function of axis position were negligible. Using a ball bar, the static XY squareness error was determined to be 8.073×10^{-4} radians. Both linear displacement errors in each of the axes and squareness errors between axes were compensated by CMM software [6]. The probe stylus was equipped with a 2.5 mm diameter spherical ruby tip. It was qualified by taking five points on a 25.0009 mm diameter precision sphere. The counter card was used to capture the scale readings of the CMM axes. Nominal tactile inspection path was created with Siemens NX 9.0. Scanner data was processed and compared using Geomagic Qualify 12.

The working principle of the blue LED structured light scanner is phase shift for 3D surface imaging [8]. A sequence of sinusoidal patterns is projected onto the object. The patterns modulated by the object surfaces are captured by the two cameras. The intensities for each pixel of the captured image are used for phase unwrapping. Finally, the unwrapped phase can be used for obtaining the depth information of the object [4]. The scanner has a vertical measurement window of 100 mm, and its near and far field of views are $60 \text{ mm} \times 105 \text{ mm}$ and $90 \text{ mm} \times 160 \text{ mm}$ respectively. Resolution ranges in X, Y, and Z axes are 0.035 – 0.108 mm, 0.090 – 0.150 mm, and 0.100 – 0.160 mm respectively, and with a maximum scan rate of 5 Hz. Its intrinsic parameters, for determining the relationship between the camera or projector coordinate system and the image coordinate system, were pre-calibrated by the manufacturer [8, 21].

3. Working principle of multi-sensor inspection system

The scanner was first calibrated with respect to the CMM. Following that, the multi-sensor synergistic inspection and oriented part inspection was performed.

3.1. Extrinsic calibration of the scanner with target

When mounted on an external device like CMM, the extrinsic parameters of the scanner have to be calibrated. That is, the Local Coordinate System (LCS) of the blue LED scanner needs to be transformed to the CMM Machine Coordinate System (MCS) [14]. To accomplish this, a target with two angled slots was conceived and manufactured (Fig. 3(a)). It is a $160 \text{ mm} \times 90 \text{ mm} \times 20 \text{ mm}$ square piece with two perpendicular 4.6 mm deep slots, each of which has a pair of symmetric 30° angled edge planes. The slots are 110 mm and 90 mm long. The width of the edge plane is 3.67 mm. The flatness, measured by taking 30 samples across the top of the target, was $24 \mu\text{m}$.

Angular misalignments between the scanner and the CMM axes were mechanically minimized first. For adjusting the roll, pitch, and yaw, a Renishaw[®] AM1 adjustment module [13] was mounted beneath the target (Fig. 3(b)). Using touch probing, the top plane of the target was adjusted to be horizontal, and the long slot to be aligned with the CMM Y axis. Another AM1 module was mounted between the scanner and the CMM Z-axis arm (Fig. 3(c)). The scanner was adjusted to align with the top plane of the target, and its Y axis with the long slot.

Following that, residual misalignments were corrected mathematically. Firstly, the top plane, the $-X$ and $+X$ 30° angled edge planes of the long slot, and the $+Y$ and $-Y$ 30° angled edge planes of the short slot were all touch probed and scanned to obtain data in the CMM MCS and the scanner LCS respectively. Secondly, using the acquired data, both the CMM MCS and the LCS of the

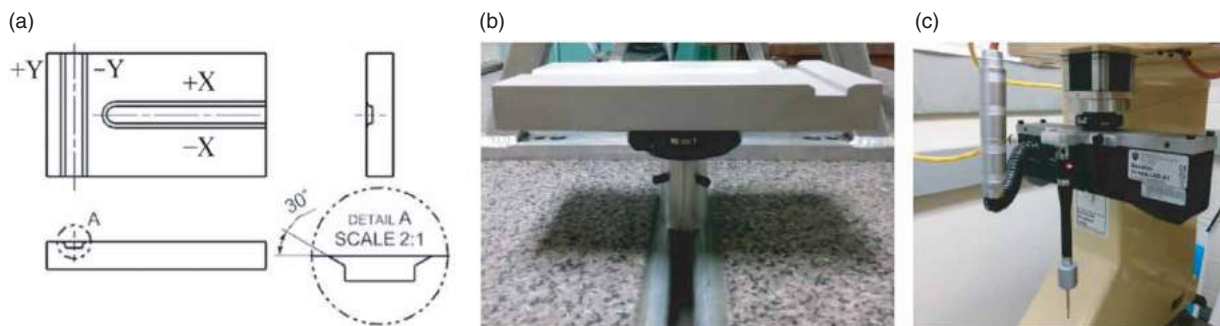


Figure 3. Calibration target and Renishaw[®] AM1 adjustment module: (a) Drawing of target, (b) Target and adjustment module, (c) Sensor and adjustment module.

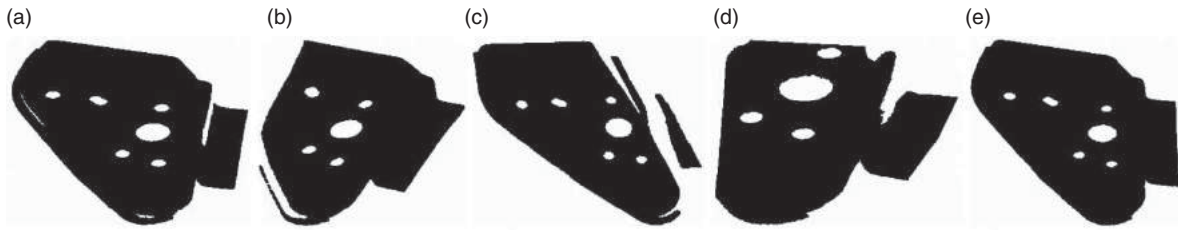


Figure 4. Digitized point clouds of the sheet metal from four orientations: (a) Horizontal, (b) $\sim +40^\circ$, (c) $\sim -40^\circ$, (d) $\sim 90^\circ$ at $\sim -40^\circ$, (e) Merged cloud of all orientations.

scanner were transformed to the calibration Target Part Coordinate System (TPCS). To construct this coordinate system, the intersection line of the two angled planes of each slot was first calculated, and projected to the top plane of the target. The intersection point of the two projected intersection lines was set as the origin. Top plane normal was set to be Z direction, and projected intersection line of long slot to be Y direction. Finally, the Homogeneous Transformation Matrix (HTM) for transforming the coordinates of the scanner LCS to the CMM MCS was obtained using Eqn. (3.1).

$$HTM_{LCS \rightarrow MCS} = HTM_{TPCS \rightarrow MCS} \times HTM_{TPCS \rightarrow LCS}^{-1} \quad (3.1)$$

3.2. Multi-sensor synergistic inspection

For synergistic inspection, features, such as holes and slots, were first measured with the blue LED sensor. The approximate geometric and dimensional properties of features obtained from the scanner were then used to adjust the nominal tactile inspection path created from CAD geometry. Finally, the features were touch probed with low uncertainty.

For single setup use, a combined blue LED scanner and touch probe CMM mechanical mount was used (Fig. 1). Software for interacting simultaneously with the counter card and the scanner was developed based on Universal Library [9] and Gocator SDK [8]. The synergistic inspection process was as follows:

- i. Calibrate the scanner with respect to the CMM using the target; obtain $HTM_{LCS \rightarrow MCS}$ (Eqn. (3.2)).

$$HTM_{LCS \rightarrow MCS} = \begin{bmatrix} R_{LCS \rightarrow MCS} & T_{LCS \rightarrow MCS} \\ 0 & 1 \end{bmatrix} \quad (3.2)$$

- ii. Manually scan a part/fixture teach point with the scanner. Transform the coordinates of the teach point from the LCS to the Global Coordinate System (GCS) of the scanner (Eqn. (3.3)).

$$P_{GCS} = R_{LCS \rightarrow GCS} \cdot P_{LCS} + P_{CMM} \quad (3.3)$$

where P_{CMM} is the scale readings of the CMM in MCS, $R_{LCS \rightarrow GCS} = R_{LCS \rightarrow MCS}$.

- iii. Using the CAD model and the information from Step 2, obtain the nominal global coordinates of the features to be measured. Position the scanner over the features, take measurement scanner snapshots, and employ the built-in scanner feature fitting software to get the approximate feature sizes and positions. Then transform the scanner data to the CMM MCS (Eqn. (3.4)).

$$P_{MCS} = HTM_{LCS \rightarrow MCS} \cdot P_{LCS} \quad (3.4)$$

- iv. Measure the same (Step 2) teach point with the touch probe, and translate the CMM MCS and the scanner data to the Part Coordinate System (PCS), the origin of which is the teach point (Eqn. (3.5)).

$$P_{PCS} = HTM_{MCS \rightarrow PCS} \cdot P_{MCS} \quad (3.5)$$

- v. Fine tune the nominal touch probing inspection path (created from the CAD nominal) using the actual scanner data, and touch probe to measure the features.

The fixture posts in Fig. 1(a) were used solely for conveniently locating the sheet metal part. There is no need to spend time measuring the posts to construct the reference coordinate system. When touch probing a hole in thin sheet metal, a common challenge is to determine the height so that measurement points are collected midway through the material thickness. With this multi-sensor approach, points on the surface around the holes were first collected using the scanner. The average height of surface points within a $1 \times 1 \text{ mm}^2$ square zone adjacent to each planned touch probe hole point was then calculated, and offset by half the material thickness to program the touch probe contact.

3.3. Rotary table and oriented part inspection

To measure surfaces with non-vertical normal, a lightweight 2-axis rotary table was designed (Fig. 1). It consists of a pair of vertical bases, suspend hangers,

locking hinges, a bottom plate, a round plate and a ring (*Lazy Susan* style) bearing. The round plate is mounted on the bearing, providing one rotary axis. The adjustable 10° angle increment locking hinges provide the second rotary axis. Three tooling spheres mounted on the table provide coordinate system registration for different table orientations.

In oriented part inspection, the part was scanned at different orientations to obtain all the top surfaces with various normal directions, and the tooling spheres were touch probed at each orientation. The scanner

data were first transformed to the CMM MCS with $HTM_{LCS \rightarrow MCS}$ (Eqn. (3.4)). The spheres centers in CMM MCS were determined using Orthogonal Least Squares [15]. After that, the HTM for registration, $HTM_{Ori \rightarrow Hor}$, was obtained by least-square fitting each oriented point set and the horizontal point set of the sphere centers [1]. Finally, the scanner data from different view angles can be merged together into the horizontal point set (Eqn. (3.6)).

$$P_{MCS}^{Hor} = HTM_{Ori \rightarrow Hor} \cdot P_{MCS}^{Ori} \quad (3.6)$$

Table 1. Measurement results of horizontal sheet metal automotive part (mm).

Hole	CAD Nominal			Blue LED			Touch Probe		
	X	Y	R	X	Y	R	X	Y	R
1	112.012	-57.300	5.000	111.839	-56.805	5.125	111.881	-56.845	4.957
						Converged	111.882	-56.842	4.957
2	101.342	-80.086	5.000	101.105	-79.688	5.126	101.131	-79.787	4.959
						Converged	101.133	-79.785	4.960
3	49.128	-58.540	5.000	49.024	-58.161	5.128	48.959	-58.268	4.949
						Converged	48.959	-58.268	4.950
4	76.738	-62.618	11.000	76.493	-62.195	11.202	76.547	-62.277	10.963
						Converged	76.547	-62.273	10.963
5	34.714	-126.508	5.000	34.739	-126.112	5.130	34.792	-126.148	4.971
						Converged	34.793	-126.148	4.971

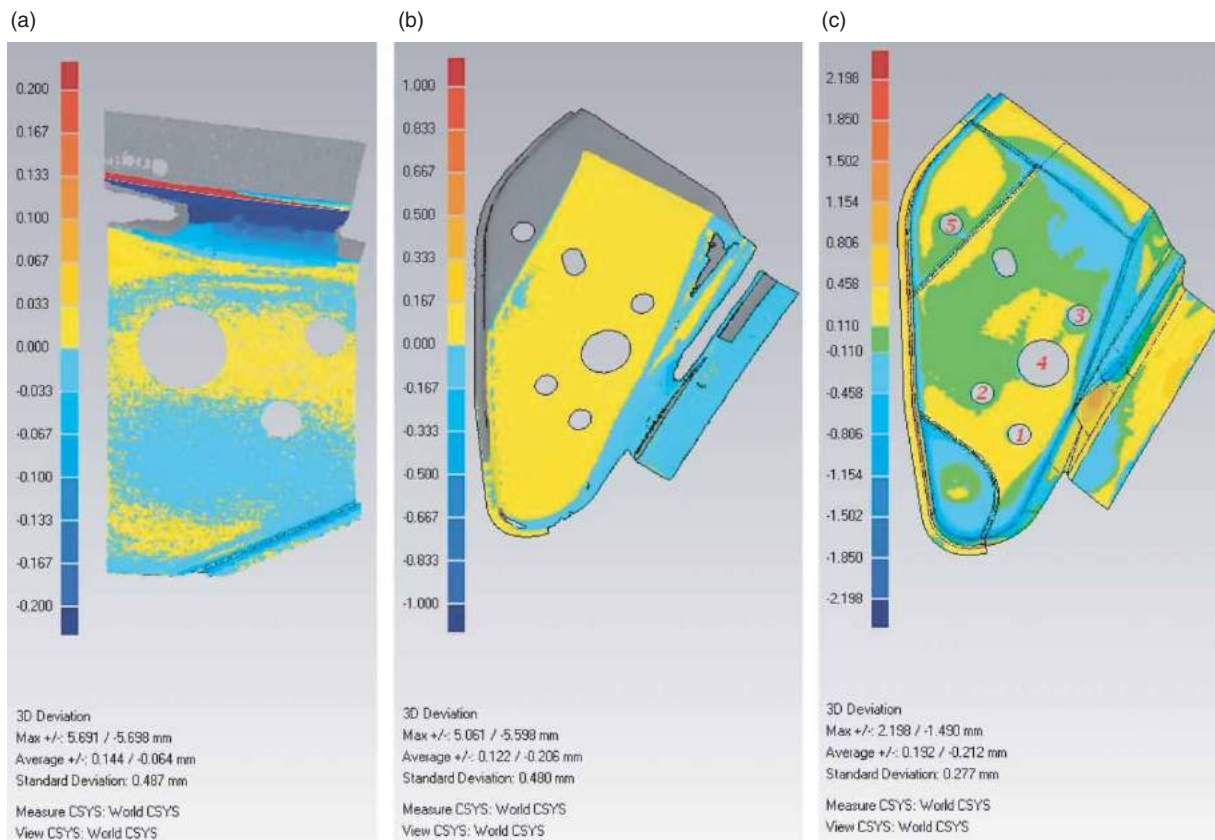


Figure 5. Scanning results of oriented part inspection (mm): (a) Horizontal point clouds comparison, (b) Horizontal and ~ +40° point clouds comparison, (c) Merged point cloud and CAD nominal comparison.

4. Experimental results

4.1. Measurement of horizontal sheet metal part with multi-sensor approach

For the horizontal table orientation, the five holes of the sheet metal automotive part were measured with this multi-sensor approach (Fig. 1(a)). The height of the scanner was adjusted to keep the part in the near view of the scanner so that highest possible resolution could be achieved. The hole positions and sizes obtained from the CAD nominal geometry, the blue LED scanner, and the touch probe are presented. The tactile measurements were iterated four times by starting with the scanner results. For brevity, only the initial and the converged tactile measurement results are shown in Tab. 1. The numbers of the holes are illustrated in Fig. 5(c). From the table, it is observed that the actual positions of the holes (the converged results) deviate as much as 0.5 mm from the CAD nominal geometry, but only up to 0.1 mm from the scanner data. Tab. 1 also indicates that even the initial tactile measurements are within 4 μm of the converged results, which implies that the iterating process can be reduced or eliminated for typical sheet metal tolerances.

Only the X and Y positions of the holes were iterated in the experiment, as the heights of the planned touch probe hole points (90° apart along X and Y directions of CMM MCS) were always determined by the scanner data as described in Section 3.2. To verify that the scanner results provided effective guidance on the height of

the hole points, the center of each adjacent square zone was touch probed. The measurement results are shown in Tab. 2. For brevity, only the results of holes 1-4 are presented. The Z values in Tab. 2 are the average height of the points in each adjacent square zone obtained by the blue LED scanner, and the height of the zone center point measured by the touch probe. As can be seen in Tab. 2, the maximum deviation between them is 0.074 mm, which is much less than the nominal 1 mm part material thickness.

4.2. Digitizing of the sheet metal at different orientations by the scanner

The sheet metal was scanned at four orientations (Fig. 4), beginning with the horizontal orientation. Using the locking hinges, the table was rotated $\sim \pm 40^\circ$. Finally, the round plate of the rotary table was rotated $\sim 90^\circ$ with the ring bearing when the table was at $\sim -40^\circ$. The tooling spheres were touch probed at each orientation, and the centers were recorded (Tab. 3). For brevity, only the sphere centers when the table was horizontal and at $\sim +40^\circ$ are presented. The corresponding registration transformation matrix was calculated and is presented.

Several snapshots were taken to cover the whole part when the table was horizontal. The point clouds of two snapshots were compared with software Geomagic Qualify 12 [5] (Fig. 5(a)). The deviations of points in regions of interest are within 0.033 mm. The points of large deviation gather on the inclined sculptured surface because its normal direction is non-vertical. The horizontal and $\sim +40^\circ$ point clouds were also compared (Fig. 5(b)). Each of them was thinned to be an evenly spaced set of points before comparison to avoid overlapped areas. The deviations of points in regions of interest are within 0.167 mm. Fig. 5(a) and 5(b) present high accuracy of $HTM_{LCS \rightarrow MCS}$ and $HTM_{Ori \rightarrow Hor}$ respectively. Finally, the point clouds of all orientations were merged together, thinned, and compared with the CAD nominal geometry (Fig. 5(c)). The deviations of the points are within 0.458 mm, except that larger deviations appear on the edge

Table 2. Measurement results of the heights of the adjacent zone points (mm).

Hole		1				2			
Adjacent Zone		1	2	3	4	1	2	3	4
Z	Blue LED	2.426	2.504	2.426	2.362	2.036	2.125	2.019	1.956
	Probe	2.355	2.443	2.376	2.295	1.974	2.051	1.974	1.908
Hole		3				4			
Adjacent Zone		1	2	3	4	1	2	3	4
Z	Blue LED	2.206	2.220	2.162	2.144	2.291	2.391	2.210	2.084
	Probe	2.147	2.156	2.128	2.094	2.224	2.317	2.161	2.032

Table 3. Tooling sphere centers and HTM for horizontal and $\sim +40^\circ$ orientations (mm).

$\sim +40^\circ$ Orientation				$HTM_{Ori \rightarrow Hor}$			
Sphere	X	Y	Z				
1	-387.313	-169.826	-64.281	1.0000	-0.0004	0.0014	0.0059
2	-515.225	-323.650	-156.448	-0.0006	0.7777	0.6286	-4.9932
3	-679.439	-243.959	-92.149	-0.0013	-0.6286	0.7777	-177.9735
Horizontal Orientation							
Sphere	X	Y	Z				
1	-387.330	-177.246	-120.684	0.0000	0.0000	0.0000	1.0000
2	-515.319	-354.734	-95.487				
3	-679.469	-252.247	-95.360				

Table 4. Distances between tooling spheres at different orientations (mm).

Orientation	Horizontal	~ +40°	~ -40°	~ 90° at ~ -40°
Distance	1-2	220.267	220.268	220.259
between	2-3	193.517	193.524	193.529
spheres	1-3	302.674	302.671	302.671
				302.706

sculptured surfaces, possibly due to actual workpiece distortion from the CAD nominal. This is currently being investigated using a separate precision analog probe equipped Zeiss Prismo [3] CMM.

The distances between the tooling spheres at the four orientations were calculated and are presented in Tab. 4. The numbers of the spheres are shown in Fig. 1(b). The maximum deviation of the distances at non-horizontal orientations from the distances when horizontal is 0.035 mm, which implies that the rotary table has high rigidity.

5. Conclusion

The multi-sensor inspection system takes advantage of both the low uncertainty of the touch probe and the high digitizing speed of the blue LED structured light scanner. The single-device structured light scanner is convenient to use and saves time for intrinsic calibration. Complementary and synergistic interactions can both be implemented in the system. The synergistic interaction of the system saves measurement time, and avoids probe collision. The angled slot calibration target can be used for calibrating the scanner with respect to the CMM. The rotary table facilitates the scanning of a surface with non-vertical normal. This system can be implemented not only on an orthogonal CMM, but also on portable CMMs and CNC machines without extensive electronic interfacing. Ongoing work will focus on refining the transformation mathematics, and further verification using an analog probe CMM.

Acknowledgements

This work was financially supported by the Natural Sciences and Engineering Research Council of Canada (NSERC) through the Canadian Network for Research and Innovation in Machining Technology (CANRIMT) and a Discovery Grant. Additional funding support was provided by Origin International Inc. (Markham, ON, CANADA), and Memex Automation (Burlington, ON, CANADA). Origin International Inc. provided the automotive sheet metal part.

ORCID

Kai Xue  <http://orcid.org/0000-0001-6391-9581>

Venu Kurella  <http://orcid.org/0000-0003-3547-7266>

Allan Spence  <http://orcid.org/0000-0002-6835-6498>

References

- [1] Arun, K.; Huang, S.; Blostein, D: Least-squares fitting of two 3-d point sets, *IEEE Transactions on Pattern Analysis and Machine Intelligence*, PAMI-9(5), 1987, 698–700. <http://dx.doi.org/10.1109/TPAMI.1987.4767965>
- [2] Barbero, B.R; Ureta, E.S: Comparative study of different digitization techniques and their accuracy, *Computer-Aided Design*, 43(2), 2011, 188–206. <http://dx.doi.org/10.1016/j.cad.2010.11.005>
- [3] Carl Zeiss Industrial Metrology, <http://www.zeiss.com/industrial-metrology>, CMM.
- [4] Geng, J: Structured-light 3D surface imaging: a tutorial, *Advances in Optics and Photonics*, 3(2), 2011, 128–160. <http://dx.doi.org/10.1364/AOP.3.000128>
- [5] 3D Systems, <http://www.geomagic.com>, Geomagic 3D software.
- [6] Hocken, R.J.; Pereira, P.H: *Coordinate Measuring Machines and Systems*, Second Edition, CRC Press, Boca Raton, FL, 2011. <http://dx.doi.org/10.1201/b11022>
- [7] Joint Committee for Guides in Metrology (JCGM): *Evaluation of Measurement Data: Guide to the Expression of Uncertainty in Measurement*, International Organisation for Standardization, Geneva, Switzerland, 2008.
- [8] LMI Technologies Inc., <http://www.lmi3d.com/>, Gocator 3110.
- [9] Measurement Computing Corporation, <http://www.mccdaq.com/>, PCI-QUAD04.
- [10] Mitutoyo America Corporation, <http://www.mitutoyo.com>, Mitutoyo GeoMeasure.
- [11] Mohib, A.; Azab, A.; ElMaraghy, H: Feature-based hybrid inspection planning: A mathematical programming approach, *International Journal of Computer Integrated Manufacturing*, 22, 2009, 13–29. <http://dx.doi.org/10.1080/09511920802382368>
- [12] Nashman, M.; Rippey, W.; Hong, T.H.; Herman, M: An integrated vision touch-probe system for dimensional inspection tasks, *National Institute of Standards and Technology - NISTIR 5678*, 1995, 1–21.
- [13] Renishaw plc, <http://www.renishaw.com>.
- [14] Santolaria, J.; Pastor, J.J.; Brose, F.J.; Aguilar, J.J: A one-step intrinsic and extrinsic calibration method for laser line scanner operation in coordinate measuring machines, *Measurement Science and Technology*, 20, 2009, 045107. <http://dx.doi.org/10.1088/0957-0233/20/4/045107>
- [15] Shakarji, C.M: Least-squares fitting algorithms of the NIST algorithm testing system, *Journal of Research of the National Institute of Standards and Technology*, 103(6), 1998, 633–641. <http://dx.doi.org/10.6028/jres.103.043>
- [16] Shen, T.S.; Jianbing, H; Menq, C.-H: Multiple-sensor integration for rapid and high-precision coordinate metrology, *IEEE/ASME Transactions on Mechatronics*, 5(2), 2000, 110–121. <http://dx.doi.org/10.1109/3516.847084>
- [17] Siemens PLM Software, <http://www.plm.automation.siemens.com>, Siemens NX 9.0.
- [18] Sladek, J.; Blaszczyk, P.M.; Kupiec, M.; Sitnik, R: The hybrid contact–optical coordinate measuring system, *Measurement*, 44, 2011, 503–510. <http://dx.doi.org/10.1016/j.measurement.2010.11.013>

- [19] Weckenmann, A.; Estler, T.; Peggs, G.; McMurtry, D: Probing systems in dimensional metrology, *CIRP Annals - Manufacturing Technology*, 53, Cmm, 2004, 657–684.
- [20] Weckenmann, A.; Kraemer, P.; Hoffmann, J: Manufacturing metrology – state of the art and prospects, 9th International Symposium on Measurement and Quality Control (9th ISMQC), 2007.
- [21] Wei, Z.; Li, C.; Ding, B: Line structured light vision sensor calibration using parallel straight lines features, *Optik - International Journal for Light and Electron Optics*, 2014.
- [22] Xie, Z.; Wang, J.; Zhang, Q: Complete 3D measurement in reverse engineering using a multi-probe system, *International Journal of Machine Tools and Manufacture*, 45, 2005, 1474–1486. <http://dx.doi.org/10.1016/j.ijmachtools.2005.01.028>
- [23] Zhao, H.; Kruth, J.P.; Van Gestel, N.; Boeckmans, B.; Bleys, P: Automated dimensional inspection planning using the combination of laser scanner and tactile probe, *Measurement: Journal of the International Measurement Confederation*, 45(5), 2012, 1057–1066.